1521-009X/44/10/1598–1602$25.00
Drug Metabolism and Disposition

http://dx.doi.org/10.1124/dmd.116.070003
Drug Metab Dispos 44:1598–1602, October 2016

Short Communication

Species Differences in Microsomal Oxidation and Glucuronidation of 4-Ipomeanol: Relationship to Target Organ Toxicity

Received February 11, 2016; accepted July 22, 2016

ABSTRACT

4-Ipomeanol (IPO) is a model pulmonary toxicant that undergoes P450-mediated metabolism to reactive electrophilic intermediates that bind to tissue macromolecules and can be trapped in vitro as the NAC/NAL adduct. Pronounced species and tissue differences in IPO toxicity are well documented, as is the enzymological component of phase I bioactivation. However, IPO also undergoes phase II glucuronidation, which may compete with bioactivation in target tissues. To better understand the organ toxicity of IPO, we synthesized IPO-glucuronide and developed a new quantitative mass spectrometry–based assay for IPO glucuronidation. Microsomal rates of glucuronidation and P450-dependent NAC/NAL adduct formation were compared in lung, kidney, and liver microsomes from seven species with different target organ toxicities to IPO. Bioactivation rates were highest in pulmonary and renal microsomes from all animal species (except dog) known to be highly susceptible to the extrahepatic toxicities induced by IPO. In a complementary fashion, pulmonary and renal IPO glucuronidation rates were uniformly low in all experimental animals and primates, but hepatic glucuronidation rates were high, as expected. Therefore, with the exception of the dog, the balance between microsomal NAC/NAL adduct and glucuronide formation correlate well with the risk for IPO-induced pulmonary, renal, and hepatic toxicities across species.

Introduction

4-Ipomeanol [IPO; 1-(3-furyl)-4-hydroxy-1-pentanone] is a furanoterpenoid toxin produced by moldy sweet potatoes (*Ipomoea batatas*), which, if ingested by livestock, can cause interstitial pneumonia, which is characterized by pulmonary edema and emphysema (Wilson et al., 1971). Beyond the poisoning of livestock, IPO is a pulmonary toxin in many laboratory animal species, which bioactivate this protoxin to a reactive intermediate that binds covalently to macromolecules predominantly in the lung (Boyd, 1976; Gram, 1989). In certain circumstances, IPO is also a renal toxin, at least in male mice (Dutcher and Boyd, 1979). IPO has also been administered to humans with the intent of treating cancer patients in whom non–small cell lung cancer was diagnosed (Christian et al., 1989). However, this proved to be unsuccessful; instead, a dose-limiting liver toxicity was observed in these patients (Rowinsky et al., 1993). Therefore, IPO-mediated toxicity exhibits species, gender, and organ selectivity.

The bioactivation of IPO may proceed via P450-mediated oxidation of the furan ring to an enedial intermediate that can be trapped by reaction with nitrogen and sulfur nucleophiles that generate a stable S-substituted pyrrole that has been fully characterized (Baer et al., 2005). The extrahepatic P450 enzyme CYP4B1 exhibits high activity for IPO bioactivation, and indeed CYP4B1 is a prominent P450 enzyme that is present in the lung of animal species that are susceptible to pulmonary toxicity (Baer and Rettie, 2006). However, IPO also undergoes extensive phase II glucuronidation (Fig. 1), at least in rats, as assessed from urine analysis (Statham et al., 1982). Therefore, to better understand the species-selective and organ-selective toxicity of IPO, we have developed a microsomal glucuronidation assay for the protoxin and use it here, together with the previously described assay for trapping the enedial, to contrast lung, liver, and kidney microsomal bioactivation and detoxification of IPO across a range of toxicity-susceptible species, including humans.

This study was supported in part by the National Institutes of Health [grant R01GM49054] and by the University of Washington School of Pharmacy Brady Fund for Natural Products.
dx.doi.org/10.1124/dmd.116.070003.

Materials and Methods

Chemicals. IPO was a gift from the National Cancer Institute (Bethesda, MD). The IPO-NAC/NAL adduct was prepared as described previously (Baer et al., 2005). NAC, NAL, CHAPS, *Escherichia coli* β-glucuronidase, silver carbonate, sodium methoxide, 4-methylumbelliferone glucuronide (4-MBG), Tris, magnesium chloride, and UDPGA were purchased from Sigma-Aldrich (St. Louis, MO). Acetobromo-α-D-glucuronic acid methyl ester was purchased from Toronto Research Chemicals (Toronto, Canada).

Biologic Materials. Pooled microsomes from male Beagle dog, male Sprague-Dawley rat, male cynomolgus monkey, and pooled mixed-gender human tissue microsomes were purchased from XenoTech LLC (Lenexa, KS). New Zealand White male rabbit tissues were obtained from R&R Research (Stanwood, WA). C57BL/6 male mice were obtained from The Jackson Laboratory (Bar Harbor, ME). Bovine tissue was from Pel-Freez Biologicals (Rogers, AR). Rabbit, mouse, and bovine liver, kidney, and lung microsomes were prepared by differential centrifugation, according to standard protocols, from tissue pooled from one to five animals.

Synthesis of IPO-Glucuronide. In a dark environment, a solution of acetobromo-α-D-glucuronic acid methyl ester (106 mg, 0.35 mmol) in dry dichloromethane (0.975 ml) was added dropwise to a suspension of IPO (23 mg, 0.14 mmol), silver carbonate (106 mg, 0.39 mmol), and 4 Å molecular sieves (40 mg) in dry dichloromethane (2.275 ml) at −40°C. After stirring for 1 hour

ABBREVIATIONS: CHAPS, 3-[(3-cholamidopropyl)dimethylammonio]-1-propanesulfonate hydrate; GST, glutathione-*S*-transferase; HRMS, high-resolution mass spectrometry; IPO, 4-ipomeanol; LC-MS/MS, liquid chromatography-tandem mass spectrometry; 4-MBG, 4-methylumbelliferone glucuronide; NAC, *N*-acetyl cysteine; NAL *N*-acetyl lysine; P450, cytochrome P450; UDPGA, uridine 5′-diphosphoglucuronic acid.

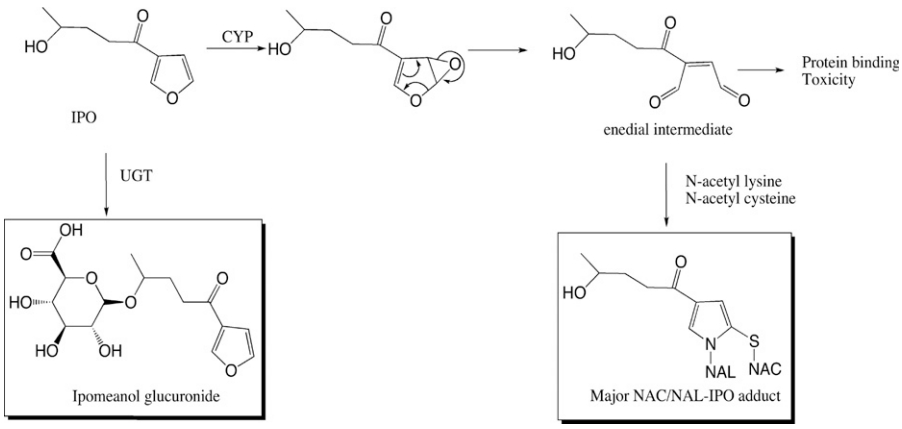

Fig. 1. Schematic illustrating bioactivation versus inactivation routes for 4-IPO after either P450- or uridine 5′-diphospho-glucuronosyltransferase-mediated metabolism.

at −40°C, the ice bath was removed, and the suspension was stirred for 24 hour The suspension was subsequently filtered through a pad of silica and washed with dichloromethane. The crude mixture was evaporated to dryness and dissolved in 3.0 ml of dry methanol followed by the addition of 0.3 ml of a 0.5 M solution of sodium methoxide in methanol. The mixture was stirred for 3 hours at room temperature and was subsequently concentrated in vacuo. Next, the crude residue was purified by silica gel chromatography (20% methanol/dichloromethane1% formic acid) to afford 9.6 mg of a pale yellow oil (20% yield over two steps). Further purification by semi-preparative chromatography afforded 98.5% pure IPO-glucuronide as a mixture of diastereomers.

NMR Spectroscopy and High-Resolution Mass Spectrometry of the Synthesized IPO Glucuronide. ^{1}H NMR spectra were obtained on an Agilent 500 MHz NMR spectrometer. Proton chemical shifts (δ) are reported in ppm from an internal standard of methanol (3.31). Coupling constants (J) are reported in Hertz, and proton chemical data are reported as follows (where s = singlet, d = doublet, t = triplet, q = quartet, m = multiplet, br = broad, ovlp = overlapping): ^{1}H NMR (500 MHz, CD_3OD), δ (in ppm): 1.22 (d, J = 6.4 Hz, 3H), 1.28 (d, J = 5.87 Hz, 3H), 1.81–1.94 (m, 4H), 2.85–2.97 (m, 1H), 3.00 (t, J = 7.6 Hz, 2H), 3.10 (t, J = 7.6 Hz, 1H) 3.13–3.18 (m, 1H), 3.23 (t, J = 7.6 Hz, 1H), 3.41 (d, J = 8.8 Hz, 2H), 3.44–3.50 (m, 2H), 3.64 (d, J = 8.31 Hz, 2H), 3.84–4.01 (m, 2H), 4.36 (dd, J = 14.2, 7.83 Hz, 2H), 6.77 (s, 2H), 7.56 (s, 1H), 7.58 (s, 1H), 8.38 (s, 1H), and 8.43 (s, 1H). High-resolution mass spectrometry (HRMS) was acquired on a Thermo Fisher LTQ Orbitrap equipped with an electrospray ionization probe. HRMS (ESI) was calculated for $C_{15}H_{19}O_9$ $[M\text{-}H]^-$ at 343.1024 (found 343.1033, error 2.6 ppm).

Enzymatic Assay for Glucuronidation of IPO. IPO glucuronidation was measured following incubation of microsomal preparations (0.1 mg protein) in triplicate with IPO (50 μM), Tris buffer (100 mM, pH 8.4), UDPGA (5 mM), CHAPS (0.5 mg/ml), and magnesium chloride (10 mM). After 60 minutes at 37°C in a shaking water bath, 250-μl reactions were terminated by the addition of an equal volume of ice-cold methanol containing the internal standard, 4-MBG, and centrifuged for 10 minutes at 4000 rpm to remove protein.

Mass Spectrometry Analysis of IPO-Glucuronide. Formation of IPO-glucuronide was measured by liquid chromatography-tandem mass spectrometry (LC-MS/MS) using the same instrument, chromatographic column, mobile phases, and gradient elution described earlier for analysis of the NAC/NAL adduct (Parkinson et al., 2013). Under these conditions, IPO-glucuronide, monitored by fragmentation of the parent sodiated glucuronide to the aglycone fragment m/z 367 → 191, with a cone voltage of 35 V and collision energy of 22 V, eluted at 4.77 minutes. The internal standard, 4-MBG, eluted at 4.61 minutes and was monitored by the transition m/z 375 → 199 with a cone voltage of 30 V and collision energy of 15 V. Using this assay, the limit of quantitation for IPO-glucuronide activity was 8 pmol/mg/60 minutes.

***β*-Glucuronidase Treatment of UDPGA-Supplemented Microsomal Incubations.** Rabbit liver uridine 5′-diphospho-glucuronosyltransferase incubations were treated with an equal volume of potassium phosphate buffer (100 mM) pH 6.0 to adjust the pH of the incubation to ~6.8. Fifty units of β-glucuronidase was added, and the mixture was incubated for 60 minutes at 37°C in a shaking water bath in a final reaction volume of 500 μl. Reactions were terminated by the addition of an equal volume of ice-cold methanol containing 4-MBG and centrifuged for 10 minutes at 4000 rpm to remove protein. Samples were then analyzed for IPO-glucuronide as described above.

Assay for Bioactivation of IPO. In vitro bioactivation of IPO was measured after a 20-minute incubation of microsomal preparations (0.1 mg of protein, 250-μl final volume) in triplicate with IPO (50 μM), with mass spectrometry analysis of the NAC/NAL adduct, as described previously (Parkinson et al., 2013). Fragmentation of the NAC/NAL adduct was monitored at m/z 452 → 353 by LC-MS/MS on a Micromass Quattro II Tandem Quadrupole Mass Spectrometer (Waters, Milford, MA) operating in electrospray-positive mode coupled to a LC system (Shimadzu, Kyoto, Japan) using a Thermo Hypersil gold 100 × 2.1 mm column with a particle size of 3 μm. Samples were eluted with 10 mM formic acid in water (aqueous phase, solvent A) and 10 mM formic acid in methanol (organic phase, solvent B) at a flow rate of 300 μl/minute. The initial conditions were 70% solvent A and 30% solvent B, which increased to 100% solvent B between 2 and 4 minutes and remained at 100% solvent B until the end of the run at 5 minutes. Under these conditions, the NAC/NAL-IPO adduct was eluted at 4.7 minutes at a cone voltage of 65 V and collision energy of 30 V, and the internal standard, furafylline (m/z 261.3 → 80.5), was eluted at 4.55 minutes, at a cone voltage of 35 V and collision energy of 25 V.

Results and Discussion

Study Design. We assessed lung, kidney, and liver microsomal IPO bioactivation to the NAC/NAL adduct and the competing reaction of IPO-glucuronidation in a wide variety of species, including common laboratory animals (mouse and rabbit), human and nonhuman primates, toxicology species used in preclinical testing of new drug entities (rat and dog) and livestock that are the target of unintentional poisoning due to the consumption of moldy sweet potatoes (bovine). A substrate concentration of 50 μM was chosen for all studies because this plasma concentration, which is relevant to human liver toxicity at least, was achieved in early human cancer studies (Rowinsky et al., 1993; Lakhanpal et al., 2001). Extended incubation times, up to an hour for the glucuronidation assays, were chosen to facilitate direct comparisons of highly varying levels of ipomeanol glucuronidation across multiple tissues and multiple animal species.

Validation of IPO-Glucuronide Metabolite. IPO-glucuronide was synthesized using a standard Koenigs-Knorr reaction between IPO and acetobromo-α-D-glucuronic acid methyl ester. After deprotection of the ester groups and column purification, IPO-glucuronide was isolated in high purity. ^{1}H NMR spectra and HRMS data for the synthetic product conform to the IPO-glucuronide structure. Supplementation of rabbit liver microsomes with UDPGA and IPO led to the formation of a metabolite at 4.82 minute (Fig. 2A). This peak, which cochromatographed with the synthetic glucuronide standard, was abolished in the absence of cofactor (Fig. 2B) and when the sample was pretreated with β-glucuronidase (Fig. 2C).

IPO Glucuronidation in Liver, Kidney, and Lung Tissues. The highest rates of IPO glucuronidation were found in liver microsomes of all species examined but with high interspecies variability (Fig. 3A).

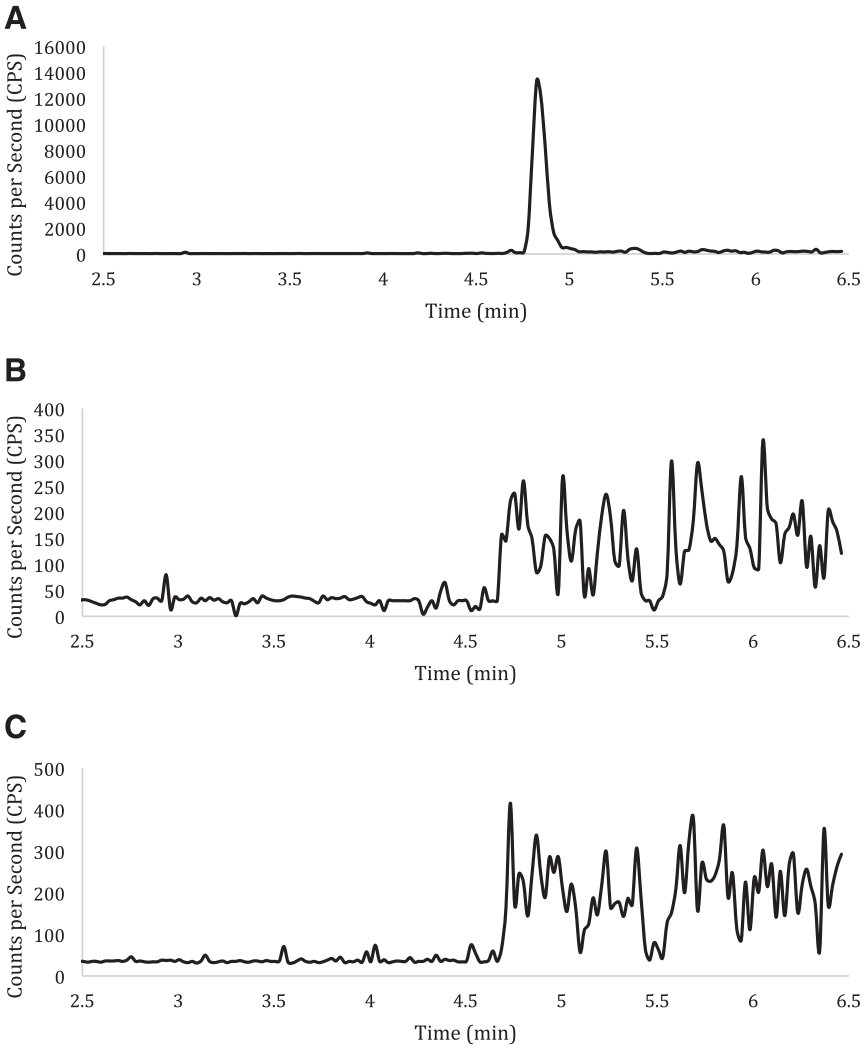

Fig. 2. Extracted ion chromatograms (*m/z* 367 → 191) for microsomal IPO-glucuronide formation by rabbit liver microsomes analyzed as detailed in *Materials and Methods*. The *x*-axis and *y*-axis are time and ion abundance, respectively. (A) Chromatogram of IPO-glucuronide formation by rabbit liver microsomes coincubated with UDPGA and CHAPS. (B) Chromatogram from rabbit liver microsomal incubations lacking UDPGA. (C) Chromatogram obtained after postincubation treatment of complete rabbit liver incubations with β-glucuronidase.

Hepatic glucuronidation rates were highest in mouse, rat, and rabbit liver, and much lower in cow, dog, monkey, and human liver. The highest rate of extrahepatic glucuronidation occurred in rabbit kidney, but this still represented only some 13% of the rate measured in rabbit liver. Several extrahepatic rates of IPO glucuronidation were close to or below the limit of quantitation at this substrate concentration. In experimental animals, lung is the principal target organ for toxicity, but the IPO glucuronidation rates are uniformly low relative to hepatic rates. In male mice, kidney toxicity is also well established, secondary to the high rates of bioactivation in this organ (Parkinson et al., 2013), where we also find IPO glucuronidation to be negligible.

IPO Bioactivation in Liver, Kidney, and Lung Tissues. In contrast to pulmonary glucuronidation, high rates of IPO bioactivation were measured in lung microsomes from most species, including those known to be susceptible to pulmonary toxicity (e.g., cow, rat, mouse, and rabbit) (Fig. 3B). The exception was the beagle dog, where, comparatively, very low rates of lung microsomal activity were detected. Human lung bioactivation was also minimal, but this is to be expected since native human CYP4B1 is an unstable enzyme with minimal activity toward IPO (Wiek et al., 2015). Kidney bioactivation of IPO was near baseline in all species examined except male mice, where the rates of NAC/NAL adduct formation were the highest recorded. This is in line with the pronounced androgen-driven expression of CYP4B1 in mouse kidney (Isern and Meseguer, 2003) and the known nephrotoxicity of IPO in this species (Dutcher and Boyd, 1979). IPO bioactivation rates in liver microsomes from lung toxicity-susceptible species were lower than in the corresponding lung microsomes, again in all cases except the dog.

IPO has long served as a model compound for studying the role of reactive intermediates in chemical pneumotoxicity. Studies using radiolabeled IPO to monitor covalent binding to microsomes demonstrated good rank order correlations between the extent of covalent binding and target tissue toxicity, especially across tissues from a given species (Dutcher and Boyd, 1979; Slaughter et al., 1983). These seminal observations were consistent with the generation of a highly reactive intermediate of IPO within the tissues where toxicity was manifest. It is now apparent that a major catalyst of IPO bioactivation is the extrahepatic P450 enzyme CYP4B1, whose paralogs across many species are present at high concentration in the lung (and male mouse kidney), but not in the liver (Baer and Rettie, 2006; Parkinson et al., 2012; Parkinson et al., 2013). Despite these strong associations between P450-mediated bioactivation of IPO by CYP4B1 and target tissue toxicity, and the attractiveness of a tissue-specific form of P450 to explain species variation in target organ selectivity of IPO, alternative pathways for the metabolism of IPO need to be considered (Connelly and Bridges, 1986). Whereas substantial progress has been made on the detailed enzymology of IPO bioactivation, very little has been established for routes of detoxification of the parent compound. It is known that IPO glucuronide is a major urinary metabolite of this

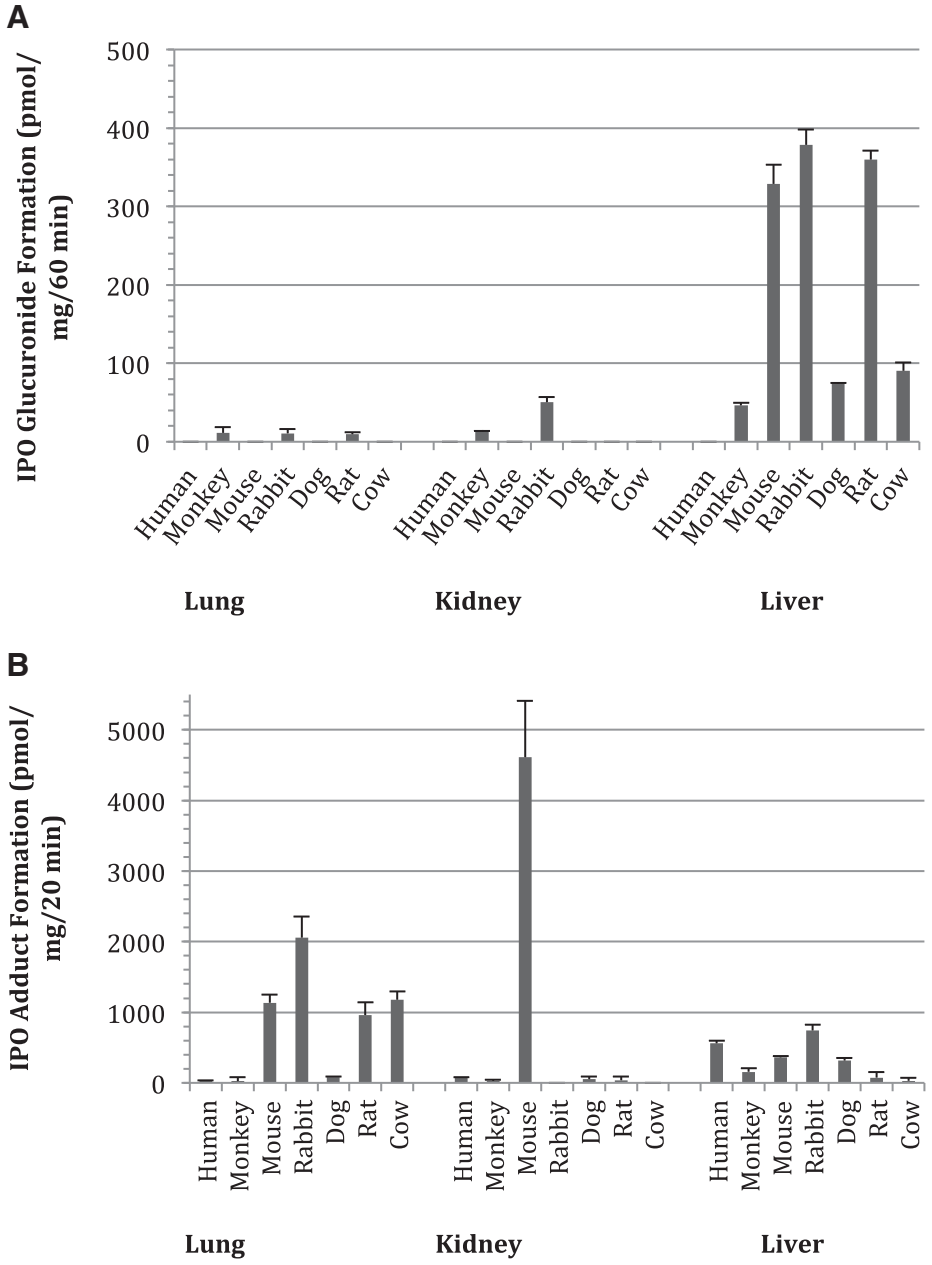

Fig. 3. Tissue- and species-selective IPO glucuronidation (A) and NAC/NAL formation (B). Metabolites were generated in microsomal incubations and analyzed by LC-MS/MS as described in the *Materials and Methods* section. To better enable comparisons of reaction velocities across multiple species and tissue with hugely different IPO bioactivation and glucuronidation capacities, microsomal incubations were conducted for extended times, up to 60 minutes for IPO glucuronidation. Note that the *y*-axis scales for the two panels are very different. Therefore, for reference and to facilitate comparisons of tissue rates for the two reactions from the graph, the lowest quantified rate of glucuronidation was 9.4 pmol/mg/60 minutes for rat lung microsomes. The lowest quantified rate of IPO adduct formation was 22 pmol/mg/20 minutes for monkey lung microsomes.

protoxin in rats (Statham et al., 1982), and one that is likely upregulated by phenobarbital treatment to the extent that it may reduce pulmonary covalent binding and lethality in this rodent species (Statham and Boyd, 1982). Therefore, the main goal of this article was to characterize both microsomal glucuronidation and oxidative bioactivation of IPO in toxicity-susceptible species and humans to evaluate the balance between these competing pathways.

The data presented here demonstrate that the in vitro NAC/NAL bioactivation assay is generally predictive of the site of IPO toxicity across most species and target organs. The high level of IPO bioactivation in pulmonary microsomes in all species relative to bioactivation in liver microsomes (with the notable exception of the dog) correlates well with the reported species selectivity regarding pulmonary toxicity. The new microsomal glucuronidation data strongly complement the bioactivation data by underlining the fact that competing pulmonary glucuronidation is minimal in all species examined. Moreover, renal glucuronidation in male mice is also inefficient in comparison with bioactivation of the toxin in this organ.

In humans, administration of IPO to lung cancer patients in the 1990s failed to precipitate the desired lung toxicity (Rowinsky et al., 1993), and instead a dose-limiting liver toxicity was observed (Lakhanpal et al., 2001). If the liver toxicity reported in humans was related to P450-mediated metabolism of IPO in that organ, the relative tissue microsomal bioactivation and glucuronidation profiles reported here would also seem to be predictive for hepatotoxicity. However, this is likely to be overly simplistic, as these microsomal experiments do not take into account potential metabolic quenching of the reactive species by other enzymes, such as cytosolic glutathione-*S*-transferase (GST). Variable GST activity can also be a critical factor in dictating chemically induced organ toxicities across species, as exemplified by aflatoxin-induced liver toxicity that is evident in rats, but not mice. In this classic case, the species difference could be attributed to differential GST activities

toward aflatoxin epoxide (Ramsdell and Eaton, 1990). Future studies that evaluate IPO bioactivation in more complex biologic milieus (e.g., S9 fractions) may help to further refine our understanding of species differences in the target organ toxicity of IPO.

Departments of Medicinal Chemistry (O.T.P., A.M.T., D.W., A.E.R.) and Pharmaceutics (E.J.K.), University of Washington, Seattle, Washington

Oliver T. Parkinson
Aaron M. Teitelbaum
Dale Whittington
Edward J. Kelly
Allan E. Rettie

Authorship Contributions

Participated in research design: Parkinson, Teitelbaum, Kelly, Rettie

Conducted experiments: Parkinson, Teitelbaum, Wittington

Contributed new reagents or analytic tools: Teitelbaum

Wrote or contributed to the writing of the manuscript: Parkinson, Teitelbaum, Kelly, Rettie

References

Baer BR and Rettie AE (2006) CYP4B1: an enigmatic P450 at the interface between xenobiotic and endobiotic metabolism. *Drug Metab Rev* **38**:451–476.

Baer BR, Rettie AE, and Henne KR (2005) Bioactivation of 4-ipomeanol by CYP4B1: adduct characterization and evidence for an enedial intermediate. *Chem Res Toxicol* **18**:855–864.

Boyd MR (1976) Role of metabolic activation in the pathogenesis of chemically induced pulmonary disease: mechanism of action of the lung-toxic furan, 4-ipomeanol. *Environ Health Perspect* **16**:127–138.

Christian MC, Wittes RE, Leyland-Jones B, McLemore TL, Smith AC, Grieshaber CK, Chabner BA, and Boyd MR (1989) 4-Ipomeanol: a novel investigational new drug for lung cancer. *J Natl Cancer Inst* **81**:1133–1143.

Connelly JC and Bridges JW (1986) Species variation in target organ toxicity, in *Target Organ Toxicity* (Cohen GM, ed) vol 1, pp 89–120, CRC Press, Boca Raton.

Dutcher JS and Boyd MR (1979) Species and strain differences in target organ alkylation and toxicity by 4-ipomeanol. Predictive value of covalent binding in studies of target organ toxicities by reactive metabolites. *Biochem Pharmacol* **28**:3367–3372.

Gram TE (1989) Pulmonary toxicity of 4-ipomeanol. *Pharmacol Ther* **43**:291–297.

Isern J and Meseguer A (2003) Hormonal regulation and characterisation of the mouse Cyp4b1 gene 5′-flanking region. *Biochem Biophys Res Commun* **307**:139–147.

Lakhanpal S, Donehower RC, and Rowinsky EK (2001) Phase II study of 4-ipomeanol, a naturally occurring alkylating furan, in patients with advanced hepatocellular carcinoma. *Invest New Drugs* **19**:69–76.

Parkinson OT, Kelly EJ, Bezabih E, Whittington D, and Rettie AE (2012) Bioactivation of 4-Ipomeanol by a CYP4B enzyme in bovine lung and inhibition by HET0016. *J Vet Pharmacol Ther* **35**:402–405.

Parkinson OT, Liggitt HD, Rettie AE, and Kelly EJ (2013) Generation and characterization of a Cyp4b1 null mouse and the role of CYP4B1 in the activation and toxicity of Ipomeanol. *Toxicol Sci* **134**:243–250.

Ramsdell HS and Eaton DL (1990) Mouse liver glutathione S-transferase isoenzyme activity toward aflatoxin B1-8,9-epoxide and benzo[a]pyrene-7,8-dihydrodiol-9,10-epoxide. *Toxicol Appl Pharmacol* **105**:216–225.

Rowinsky EK, Noe DA, Ettinger DS, Christian MC, Lubejko BG, Fishman EK, Sartorius SE, Boyd MR, and Donehower RC (1993) Phase I and pharmacological study of the pulmonary cytotoxin 4-ipomeanol on a single dose schedule in lung cancer patients: hepatotoxicity is dose limiting in humans. *Cancer Res* **53**:1794–1801.

Slaughter SR, Statham CN, Philpot RM, and Boyd MR (1983) Covalent binding of metabolites of 4-ipomeanol to rabbit pulmonary and hepatic microsomal proteins and to the enzymes of the pulmonary cytochrome P-450-dependent monooxygenase system. *J Pharmacol Exp Ther* **224**:252–257.

Statham CN and Boyd MR (1982) Effects of phenobarbital and 3-methylcholanthrene on the in vivo distribution, metabolism and covalent binding of 4-ipomeanol in the rat; implications for target organ toxicity. *Biochem Pharmacol* **31**:3973–3977.

Statham CN, Dutcher JS, Kim SH, and Boyd MR (1982) Ipomeanol 4-glucuronide, a major urinary metabolite of 4-ipomeanol in the rat. *Drug Metab Dispos* **10**:264–267.

Wiek C, Schmidt EM, Roellecke K, Freund M, Nakano M, Kelly EJ, Kaisers W, Yarov-Yarovoy V, Kramm CM, Rettie AE, et al. (2015) Identification of amino acid determinants in CYP4B1 for optimal catalytic processing of 4-ipomeanol. *Biochem J* **465**:103–114.

Wilson BJ, Boyd MR, Harris TM, and Yang DT (1971) A lung oedema factor from mouldy sweet potatoes (Ipomoea batatas). *Nature* **231**:52–53.

Address correspondence to: Allan E. Rettie, Box 357610, School of Pharmacy, University of Washington, Seattle, WA 98195-7610. E-mail: rettie@uw.edu